Available online at www.sciencedirect.com
ScienceDirect
Polymer 49 (2008) 2107–2114
polymer
www.elsevier.com/locate/polymer

Photorefractive properties of polyphosphazenes containing carbazole-based multifunctional chromophores

Li Zhang [a], Jun Shi [a], Zheng Yang [a], Maomao Huang [b], Zhijian Chen [b], Qihuang Gong [b], Shaokui Cao [a,*]

[a] School of Materials Science and Engineering, Zhengzhou University, Zhengzhou 450052, China
[b] Department of Physics, Peking University, Beijing 100871, China

Received 10 June 2007; received in revised form 24 August 2007; accepted 26 September 2007
Available online 29 September 2007

Abstract

A series of amorphous polyphosphazenes containing carbazole-based multifunctional chromophores were synthesized. These polymers show low glass transition temperature (20–65 °C) and can easily be fabricated into optically transparent films with long-term stability. As an unambiguous evidence of photorefractive effect, preliminary two-beam-coupling experiments were performed at 633 nm under room temperature. All of these single-component polymers exhibited photorefractive performance without external electric field or prepoling, and gain coefficient of 91 cm^{-1} was observed in a polymer with the lowest glass transition temperature. The influence of the alkylene spacer length between the side group and the polymer backbone on the glass transition temperature, chromophore loading, as well as the optical gain was discussed. The steady-state photorefractive performance of a polyphosphazene with the shortest alkylene spacer was enhanced significantly by adding a photoconductive plasticizer *N*-ethyl-carbazole to lower the glass transition temperature and a gain of 198 cm^{-1} and a diffraction efficiency of 46% were achieved at zero electric field.

Keywords: Photorefractive; Polyphosphazene; Post-azo-coupling

1. Introduction

Organic photorefractive (PR) materials are potentially useful for high-density optical data storage, image processing, optical computing and nondestructive testing [1]. Among various classes of PR materials, photorefractive polymers are promising since they possess outstanding and unique advantages over inorganic and organic crystals such as the highest figure of merit, versatility in structural design, and good processability [2]. To exhibit a photorefractive effect, materials should possess photoconductivity for the formation of a space-charge field and electric-optic (EO) properties for the subsequent modulation of the refractive index. There have been two approaches to incorporate these properties into polymeric materials, one is host–guest polymer composite [3,4], and the other is fully functionalized polymer [5,6]. Host–guest polymer composites normally exhibit poor stability due to phase separation. While, fully functionalized polymers are difficult to be synthesized due to the tedious and complicated procedures, in which the small amount of photo-sensitizer is normally difficult to be linked to the polymer backbone.

As a different approach, multifunctional polymers, which exhibit both photoconductivity and EO activity, have attracted growing interest because of their high stability and ease in synthesis [7–10]. In our earlier work, a series of multifunctional photorefractive polymethacrylates with azocarbazole side group have been synthesized [11,12]. However, high glass transition temperature (T_g) of these polymers made it difficult to pole at room temperature to achieve alignment of the chromophores and consequently the high value of nonlinear optical

* Corresponding author. Tel./fax: +86 371 6776 3561.
E-mail address: caoshaokui@zzu.edu.cn (S. Cao).

0032-3861/$ - see front matter © 2007 Elsevier Ltd. All rights reserved.
doi:10.1016/j.polymer.2007.09.038

(NLO) coefficient. Tuning the T_g to room temperature by adding a large amount of plasticizer always results in the deduction of photorefractive performance due to the relative low content of chromophore.

Polyphosphazenes, which contain a very flexible inorganic backbone of alternating phosphorous and nitrogen atoms, have the potential to obtain polymers with low T_g because the flexibility of the skeleton defines the maximum low-temperature elasticity that can be expected. In recent years, polyphosphazenes have been demonstrated as excellent candidates for EO applications due to their unique properties, such as high thermal and oxidative stability, optical transparency from 220 nm to the near-IR region of the backbone, and the ease of synthesis [13–16]. However, few reports were found in literature concerning photorefractive study of polyphosphazenes to date [17]. We have very recently reported that thin film of a novel carbazole-based polyphosphazene was shown to be suitable material for storage of a photorefractive grating [18]. This multifunctional polyphosphazene was prepared via post-functionalization approach, which provides the possibility of building variable spacers between the side group and the inorganic polymer backbone. Thus, various properties of polymers could be tailored, such as T_g, solubility, morphology and film-forming ability, which would directly influence the photorefractive performance.

To get further insight on the structure and property correlation, the present paper reports a series of multifunctional polyphosphazenes based on the similar carbazole side group, where the spacer length between the side group and the phosphazene main chain is systematically increased by the number of methylene groups. The photorefractive effects of these polymers were demonstrated by two-beam-coupling (TBC) as well as four-wave-mixing (FWM) measurements. We found that all of these single-component polymers exhibited PR performance at room temperature without external electric field or prepoling and the steady-state PR performance could be enhanced significantly by use of a charge-transporting plasticizer. The influence of the alkylene spacer length between the side group and the polymer backbone on the T_g, chromophore loading, morphological behavior as well as the optical gain was discussed.

2. Experimental

2.1. Instrumentation

^{1}H NMR (400 MHz) and ^{31}P NMR (162 MHz) spectra were conducted with a Bruker DRX-400 NMR spectrometer using $CDCl_3$ as solvent. IR spectra were recorded on a Nicolet-460 FTIR spectrometer on KBr pellets. UV–vis spectra were recorded with a Shimadzu 3010 UV–visible spectrometer using THF as solvent and mole concentration of all samples was 0.1 mmol/L. Elemental analysis was measured with an MOD-1106 elemental analysis system. Gel permeation chromatography (GPC) analysis was performed on HLC-8220 liquid chromatograph with THF as eluent and UV/RI detection versus polystyrene standards. Differential scanning calorimetry (DSC) analysis was carried out under nitrogen on TA-2920 differential scanning calorimeter at a heating rate of 10 °C/min. Thermogravimetric analysis (TGA) was performed on a Netzsch-209 TGA system at a heating rate of 10 °C/min.

2.2. Materials

All materials were commercially available and used as received except that the solvents were purified before use. Tetrahydrofuran (THF) was dried over and distilled from calcium hydroxide under an atmosphere of dry nitrogen. Compound **1**, hexachlorocyclotriphosphazene, was synthesized from ammonium chloride and phosphoric chloride following literature procedure [19]. Compounds **2**–**4** were prepared by the reaction between carbazole and corresponding ω-chloro- or ω-bromo-alcohol in dimethylformamide (DMF) in the presence of potassium hydroxide as a hydrochloride or hydrobromide acceptor [8].

2.3. Synthesis

The synthetic procedure for the polymers is summarized in Scheme 1. Polymer **P1**, poly(dichlorophosphazene), was first prepared via ring-opening polymerization from hexachlorocyclotriphosphazene. Then, polyphosphazenes **P2**, **P3** and **P4** with carbazole side groups were subsequently prepared by the substitution of chloro groups in polymer **P1** with a carbazole compound, which was carried out in a dry argon atmosphere. Finally, the target polymers **P5**, **P6** and **P7** were obtained via an azo coupling reaction, in which the carbazole ring was partially functionalized with a nitrophenyl azo group. The detailed synthesis of polymers **P1**, **P3** and **P6** [18], and that of polymers **P4** and **P7** [20] can be found in our earlier publications. Polymers **P2** and **P5** were synthesized in similar procedures with those of **P3** and **P6**.

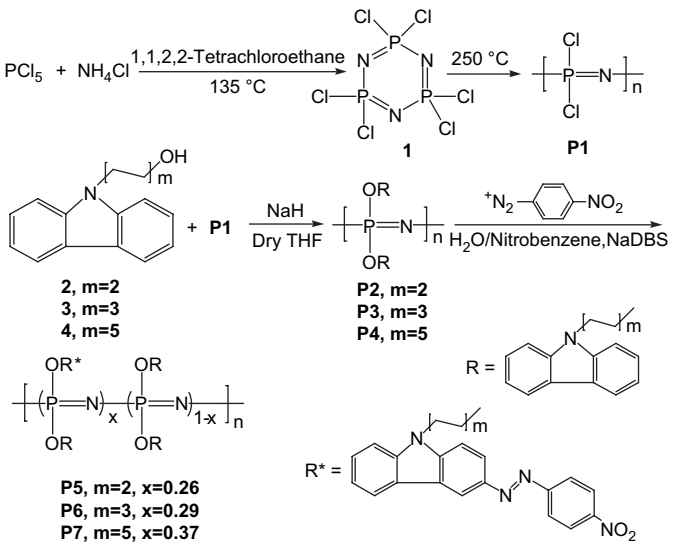

Scheme 1. Synthetic routes for photorefractive polyphosphazenes.

*2.3.1. Preparation of polyphosphazene **P2***

N-[4′-(Hydroxybutyl)]-carbazole (5.88 g, 24.6 mmol) was allowed to react with sodium hydride (1.2 g, 30 mmol) in THF (60 mL) at reflux for 24 h. Then, 20 mL of THF solution of polymer **P1** (0.65 g, 11.2 mmol) was added. The mixture was stirred at reflux for 48 h, and was poured into water (500 mL). The precipitate was filtrated, washed with water, and air-dried. The product was purified by succeeding re-precipitations of THF solution from water, methanol and hexane, respectively. A white powdery product **P2** was obtained after drying in vacuum at 40 °C. Yield: 1.4 g, 47%. ^{1}H NMR ($CDCl_3$): δ (ppm) 7.8 (s, 2H, ArH), 7.0–6.9 (d, 4H, ArH), 6.7 (s, 2H, ArH), 3.4–3.2 (d, 4H, NCH_2, CH_2O), 1.1–0.7 (m, 4H, $(CH_2)_2$); ^{31}P NMR ($CDCl_3$): δ (ppm) −8.96 (s). IR (KBr, cm^{-1}): 3048, 1597, 1484, 1452 (carbazole); 2948 (alkyl-H); 1327, 1231 (P═N); 1050 (P–O–C); 749, 722 (P–N). Anal. Calcd: C, 73.69; H, 6.18; N, 8.06. Found: C, 73.81; H, 5.98; N, 7.92.

*2.3.2. Preparation of polyphosphazene **P5***

4-Nitroaniline (0.28 g, 2 mmol) was dissolved in a solution of concentrated HCl (20 mL). The mixture was cooled with an ice bath to lower than 4 °C, and then an aqueous solution containing sodium nitrite (0.16 g, 2.4 mmol) was slowly added. The mixture was allowed to stir in the ice bath for 30 min. Sodium dodecylbenzenesulfonate (NaDBS) (0.2 g) and a solution of **P2** (0.52 g, 2 mmol of carbazole groups) in nitrobenzene (20 mL) were successively added. The reaction mixture was stirred vigorously at room temperature for 30 h, and then another part of diazonium salt prepared from 2 mmol of 4-nitroaniline and 0.16 g of sodium nitrite was added. After stirring vigorously at room temperature for another 30 h, the reaction mixture was washed with water, and then poured into cold methanol to precipitate the product. The precipitate was filtered and dried, then purified by re-precipitation of a THF solution from methanol for three times. An orange solid (0.34 g) was obtained after drying in vacuum at 40 °C. ^{1}H NMR ($CDCl_3$): δ (ppm) 8.4–6.7 (m, ArH), 3.3 (s, NCH_2, CH_2O), 1.7–0.7 (m, $(CH_2)_2$); ^{31}P NMR ($CDCl_3$): δ (ppm) −8.50 (s). IR (KBr, cm^{-1}): 1595 (N═N); 1520, 1340 (NO_2); 856 (phenyl-H).

2.4. Photorefractive sample preparation

For the photorefractive measurements, single-component polymer films of **P5**, **P6** and **P7** were prepared as follows. Polymers were dissolved in THF (10 wt%) and the solutions were filtered through a 0.2 μm pore Teflon membrane filter and then dipped onto two indium tin oxide (ITO) glass plates at room temperature. Residual solvent was removed by heating the film at around T_g in vacuum for 12 h. The dried sample was warmed on a hot plate and then the melted sample was sandwiched between the two ITO glass plates by applying gentle pressure. The sandwich was cooled quickly to room temperature while maintained under pressure and the thickness of the film was controlled to be 80 μm through a Teflon spacer. The polymer composite sample consisted of 90 wt% of **P5** and 10 wt% of *N*-ethyl carbazole (ECZ) was also fabricated by the same procedure. All the resultant sample films were of satisfactory optical quality.

2.5. Photorefractive measurements

The PR effect of 80 μm-thick films of polymers was measured by two-beam-coupling and four-wave-mixing experiments [1] employing an oblique geometry as shown in Fig. 1. Two coherent *p*-polarized He–Ne laser beams at a wavelength of 633 nm overlapped in the sample to produce an interference pattern. The normal of the sample surface was tilted at an angle $\phi_{ext} = 35°$ (in air) with respect to the symmetric axis of the two incident beams, and the angle between the two writing beams $2\theta_{ext} = 20°$ (in air). In the TBC experiment, the initial power of two writing beams (beam 1 and beam 2) was measured to be 15 and 10 mW, respectively. The TBC coefficient Γ could be estimated from the following expression [21,22]:

$$\Gamma = \frac{\cos\phi_{in}}{d}\left(\ln(\gamma_0\beta) - \ln(\beta + 1 - \gamma_0)\right)$$

where $d = 80$ μm is the thickness of the sample, ϕ_{in} is the incident angle of the beam 1 inside the sample, β is the initial intensity ratio of beams after the sample (in the absence of coupling), and $\gamma_0 = I/I_0$ is the beam coupling ratio where I_0 is the signal intensity without the pump beam, and I is the signal intensity with the pump beam.

For the FWM experiment, two *p*-polarized beams with the same intensity of 10 mW were used as writing beams. An

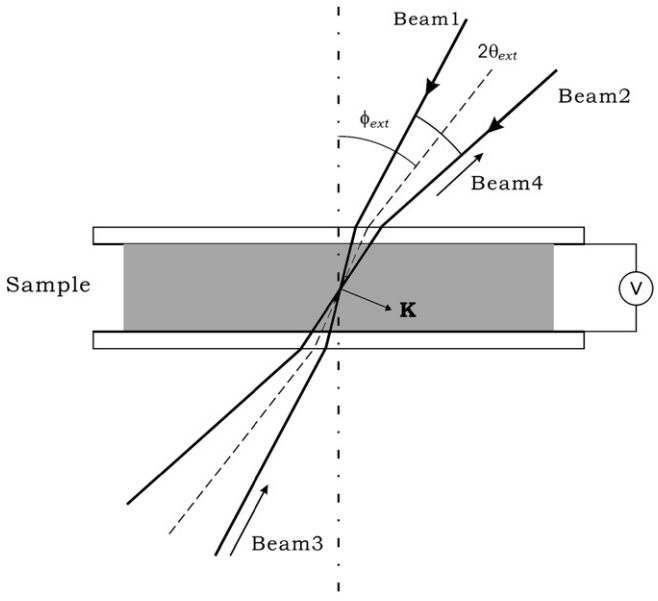

Fig. 1. Experimental setup for two-beam coupling and four-wave mixing. Only beam 1 and beam 2 are present in two-beam coupling experiment, which are *p*-polarized He–Ne laser beams. Beam 3 is the *s*-polarized probe beam and beam 4 is the diffractive beam. $\phi_{ext} = 35°$ is the tilted angle of the symmetric axis of the two incident beams with respect to the sample normal, and $2\theta_{ext} = 20°$ is the external interbeam angle. **K** is the grating wave vector. *V* is an applied external electric field.

s-polarized probe beam 3 with the intensity of 0.5 mW counterpropagated to writing beam 1 and the diffracted beam intensity was measured in the reverse direction of writing beam 2. Diffraction efficiency was determined by the ratio of the intensity of diffracted signal to that of incident reading beam.

All the photorefractive measurements were employed on the unpoled samples under room temperature.

3. Results and discussion

3.1. Synthesis of polyphosphazenes

As shown in Scheme 1, precursor polymers **P2**, **P3** and **P4** were obtained from the highly reactive macromolecular intermediate polymer **P1**, poly(dichlorophosphazene), by nucleophilic substitution reaction, which took place by the addition of a solution of **P1** in dry THF to an excess amount of the sodium alkoxide nucleophile of the corresponding carbazole compounds **2**–**4**, and then refluxed for two days. ^{31}P NMR spectroscopy was used to monitor the progress of reaction until no further change in the spectrum occurred. The obtained polymers **P2**, **P3** and **P4** did not cross-link even after precipitations from water or exposure to atmospheric moisture, which illustrated that no residual chlorine atom in **P2**, **P3** and **P4** was remained.

Polymers **P5**, **P6** and **P7** were synthesized via post-azo-coupling reaction between precursor polymers and diazonium salts, which worked in a two phase system (nitrobenzene/water) at room temperature, using 4-sodium 4-dodecylbenzenesulfonate (NaDBS) as a phase transfer catalyst. This procedure was reported previously as giving good yields on functionalization of the well-known unreactive carbazole derivatives [11]. It was interesting to find that the amount of azo groups attached to the carbazole rings in precursor polymers could be adjusted by varying the reaction time and the diazonium salt concentration. Therefore, in order to obtain a higher chromophore loading in polymers **P5**, **P6** and **P7**, longer reaction time (60 h) and larger excess of diazonium salt were necessary. The degree of functionalization was determined by the quantitative analysis of UV–vis absorption spectra and the results are summarized in Table 2. Like other post-functionalization reactions [14,21], it is difficult to determine the exact position of electrophilic substitution on the side group along the polymeric backbone. However, owing to the bulkiness of the introduced functional group and steric effect of the azo coupling product, it is reasonable to assume that the coupling reaction took place initially on the unfunctionalized repeating unit and exclusively at the 3-position of carbazole, as shown in Scheme 1.

The length of the alkylene spacer between the side group and the polymeric backbone would give a big influence on both the degree of functionalization and the solubility of the resultant polymers. The chromophore loading in polymers **P5**, **P6** and **P7** increased with the alkylene spacer length after following the same reaction procedure, which would be attributed to the lessening of steric hindrance induced on the carbazole side group by the polymeric backbone. The resultant polymers **P5**, **P6** and **P7** showed good solubility in common organic solvents like chloroform, THF and DMF. The solubility of polymer **P7** was even more excellent presumably due to the longer alkylene spacer. Polymer films with high optical quality could be easily fabricated through solution casting.

3.2. Characterization of polyphosphazenes

The structure of polyphosphazenes **P2** and **P5** was characterized by using ^{1}H NMR, ^{31}P NMR, IR spectroscopies as well as elemental analysis, and the results are presented in the experimental part. In the ^{1}H NMR spectrum of **P5**, several new signals appeared in the downfield at around 8.4 ppm were attributed to the *p*-nitrophenyl moiety, which confirm the successful formation of the azocarbazole chromophore. A sharp singlet resonance at around −8 ppm was observed in the ^{31}P NMR spectra of **P2** and **P5**, which is typical for alkoxy-substituted polyphosphazenes. The similarity in the ^{31}P NMR spectra presumably revealed a consequence of the similar chemical environment of the phosphorus atoms in **P2** and **P5**. In addition, the singlet resonance also gave an evidence for the complete substitution of the chlorines in polymer **P1**, which was further supported by the results of elemental analysis of **P2**. IR spectrum of **P5** showed the absorptions for −N=N− at 1595 cm^{-1}, for $-NO_2$ at 1520 and 1340 cm^{-1}, and for the phenyl ring at 856 cm^{-1}.

Molecular weight (MW) of polymers **P2** through **P7** was estimated by gel permeation chromatography as shown in Table 1. The data for polymer **P3** could not be obtained because of its poor solubility in THF. All the polymers have relatively lower MW than typical molecular weight values (10^6) expected for polyphosphazenes. During the macromolecular substitution reaction of polymer **P1**, it is likely that the polymer chains are partly broken by thermally induced depolymerization for the longer reaction time and high temperature [13], despite the reactive condition would benefit to complete substitution. After the azo coupling, the MW of polymers **P5**, **P6** and **P7** increased a little compared to the precursor polymers **P2**, **P3** and **P4**, which indicated that no hydrolysis or crosslinking of the phosphazene polymer backbone happened during the post-azo coupling reaction.

Thermal analysis results for the polymers are also listed in Table 1. All samples were initially ramp-heated up to 100 °C and were then cooled quickly to −30 °C in an attempt to establish a more uniform thermal history for all the polymers.

Table 1
Molecular weights and thermal analysis for polyphosphazenes

Polymer	M_n	M_w	PDI	T_g (°C)	T_d (°C)
P2	19,400	34,700	1.8	59	276
P3	[a]	[a]	[a]	38	293
P4	8600	11,300	1.3	5	292
P5	20,300	37,000	1.8	65	277
P6	22,600	65,200	2.8	50	293
P7	10,600	12,800	1.2	20	284

[a] Information not available because of insolubility of **P3**.

No melting transition was detected in the DSC measurement except for a single glass transition, and it appears that these polymers are amorphous. It is well known that many polyphosphazenes are semi-crystalline below their T_g [16]. However, the attachment of a spacer group between the carbazole group and the main chain could reduce the ability to crystallize and improve the transparency of the polymers, presumably by decoupling the motions of the side group from those of main chain. The absence of micro-crystallinity is an important requirement for a polymer that is to be considered for uses in nonlinear optical devices. It can be observed that the T_g of the polymers was depressed with the increase in the alkylene spacer length, which suggests that there is a substantial increase in the segmental mobility from shorter spacer to longer. Compared to the T_g of precursor polymers, the conformational stiffness of the azobenzene group could contribute to polymers **P5**, **P6** and **P7** an increased T_g. However, the T_g values are still significantly lower than that of previously reported polymethacrylates containing the same NLO side group [11,12], which is primarily a consequence of the highly flexible character of the phosphazene backbone coupled with the flexible spacer group. The thermogravimetrical analysis showed that the initial decomposition temperature of the polymers were as high as 290 °C.

3.3. Absorption spectra

In order to determine the chromophore loading in polyphosphazene, a model compound with the same chromophore structure, (4-nitrophenyl)-[3-[*N*-(2-hydroxy ethyl)carbazolyl]]-diazene, was synthesized (Scheme 2) according to literature procedures [8]. Fig. 2 shows the UV–vis spectra of polymers **P4** through **P7** compared with the absorption spectrum of the model compound. The precursor polymer **P4**, with the similar UV–vis spectra to **P2** and **P3**, showed only the typical absorptions of carbazole moiety peaked at 330 and 343 nm, indicating that the phosphazene backbone has no absorption in the visible range. After the azo coupling reaction, a new broad absorbance in the range of 360–570 nm was observed for polyphosphazenes **P5** through **P7**, which was derived from the charge-transfer from carbazolyl to the nitro group. Absorption maxima of the attached multifunctional chromophores remain almost unshifted compared to the model chromophore in THF solution. The chromophore loadings of polymers **P5**, **P6** and **P7** were determined from the absorption at λ_{max} of the attached multifunctional chromophores and that of the model compound [11,23,24] and the results are listed in Table 2.

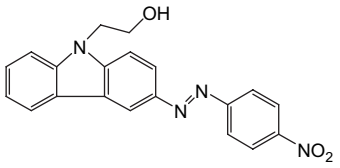

Scheme 2. Structure of model compound.

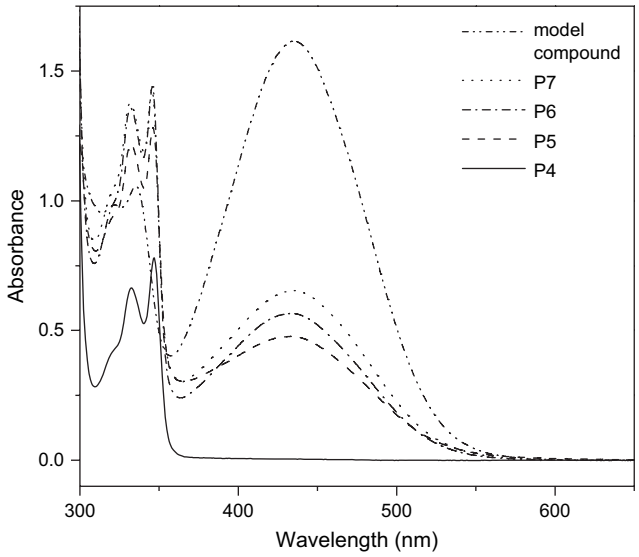

Fig. 2. UV–vis spectra of polyphosphazenes **P4** through **P7** and model compound in THF solution (0.1 mmol/L).

3.4. Photorefractive properties

3.4.1. Single-component polymer samples

Films of polymers containing azobenzene chromophores have been shown to be suitable materials for inscription of a variety of holographic gratings such as isomerization, birefringence and surface relief [8,25]. Therefore, four-wave-mixing experiments to measure the photorefractive effect by diffraction efficiency would not be conclusive. The photorefractive properties of single-component polymer samples can be verified by asymmetric TBC experiments. The nonlocal response leads to an energy exchange between the two writing beams incident on the sample, which is a signature of a photorefractive index grating and distinguishes a photorefractive index grating from other laser-induced dynamic gratings.

Measurements were first made under zero-field conditions. A typical TBC energy transfer is depicted in Fig. 3 for a sample of polymer **P7**. Energy is transferred from the weaker beam to the stronger one and the optical gain Γ can be estimated as 91 cm^{-1}. The TBC process was monitored for a long time (more than 160 min) and the energy transfer direction did not change, which eliminates the feasibility that the TBC effect is caused by the irregular movement of interference pattern with respect to local grating due to the instability of the laser-based optical system [26]. Nonzero and stable TBC

Table 2
Chromophore loadings and optical properties of PR polyphosphazenes

Polymer	λ_{max} (nm)	Loading[a]	Γ (cm^{-1})[b]
P5	433	0.26	91
P6	433	0.29	79
P7	435	0.37	50

[a] Loading indicates the average number of NLO chromophores per each repeating –P=N– unit.

[b] Measurements were made without poling and without applying an external electric field.

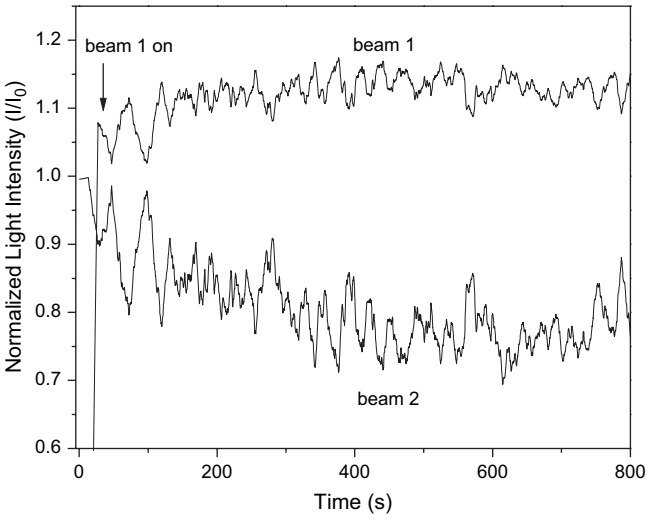

Fig. 3. TBC signal measured in **P7** at zero electric field. Beam 2 intensity (lower trace) decreased when beam 1 (upper trace) is turned on.

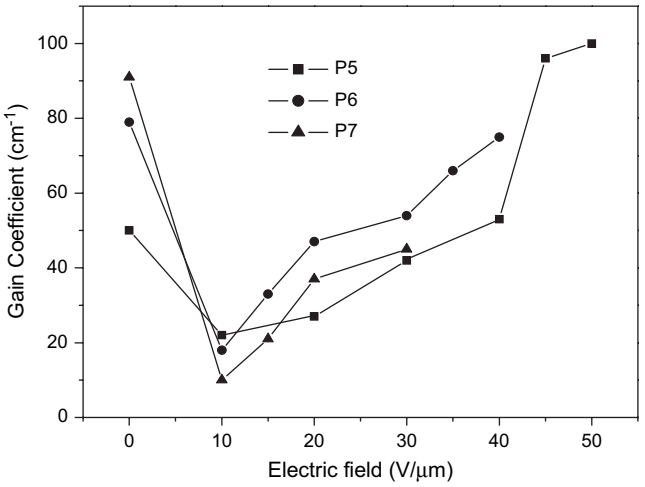

Fig. 4. TBC gain coefficient of polymers **P5**, **P6** and **P7** as a function of applied field.

signals were also observed in other single-component polymer samples at zero electric fields and the optical gains calculated from the measured energy exchange are listed in Table 2.

However, it is well known that according to PR theory an external electric field to remove inversion symmetry is necessary for PR effects in organic materials. Recently TBC gain has been reported in some PR polymeric materials without an external field or prepoling [22,27,28], but the exact mechanism of this effect still remains not so clear. It is reasonable to assume that the synergism of the photoassisted poling of azo dye and the longitudinal space-charge field may be responsible for the TBC effect observed in our polymers. Photoassisted poling effects in azo dyes have been studied by several groups [29–31]. It has been suggested that in the presence of a polarized light, the repeated *trans–cis–trans* photoisomerization can enhance the rotational mobility of the azo groups and make them rotate easily at weak electric field. When the sample is illuminated by the interference pattern, a periodic space-charge field can arise. Meanwhile, the light absorption, due to the dye, produces intensity attenuation along the light path that induces a charge displacement and hence a longitudinal space-charge field in the same direction [32]. These two kinds of space-charge fields may contribute to the local poling of the azo groups. Such an effect of breaking the symmetry by longitudinal field formation has been observed experimentally and explained theoretically in PR liquid crystal composites [33] and the possibility of observing this effect in polymeric materials was also suggested [33,34]. Nevertheless further studies are necessary for clarifying the TBC mechanism in our case.

From the values of coupling gain Γ at zero electric field, it is distinct that the samples with longer alkylene spacer experience an increase in optical gain. This could be attributed to the increased mobility of the side chains, which made it easier to achieve photoassisted poling when the sample was illuminated by polarized light, and it could also represent an increased EO effect, as samples with longer spacer bear larger chromophore loadings and hence should have a larger index modulation amplitude Δn resulting in an increased EO response.

The effect of external electric field on the TBC optical gain was also studied and the results are presented in Fig. 4. It is an interesting phenomenon that the gain coefficient of all samples reduced quickly at the beginning of applied electric field of 10 V/μm, and then increased gradually as the further increase of the external electric field. For most of photorefractive polymers, all the processes in polymers that are responsible for space-charge field build-up and chromophores orienting are strongly electric field-dependent, and as a result two-beam coupling gain frequently increases with electric field [1]. However, the effect of external electric field on 2BC gain in our case is somewhat abnormal, which needs further study for seeking an explanation. All the single-component samples show excellent phase stability and remain unabated photorefractive performance over 1 year under dark condition.

Although the Γ values of the single-component photorefractive polyphosphazenes were not as high as that of high-performance fully functionalized PR materials ($\Gamma > 200\ \mathrm{cm}^{-1}$) [1], the observation of a nonlocal grating without prepoling and without applying an external electric field suggests that a new class of photorefractive polymers could be developed, in which an oblique geometry or electric field is not necessarily required for a photorefractive response. Hence, the use of two transparent electrodes (ITO glasses) is not necessary, which greatly helps to significantly reduce optical losses due to scattering and surface reflection. Therefore, the polymers can be made thicker and subsequently a variety of fabrication methods can be employed in order to enhance the photorefractive performance. Further work for this challenge is in progress.

3.4.2. Polymer composite sample

Generally, an increase in temperature that is below T_g leads to improved PR properties due to an enhanced orientational

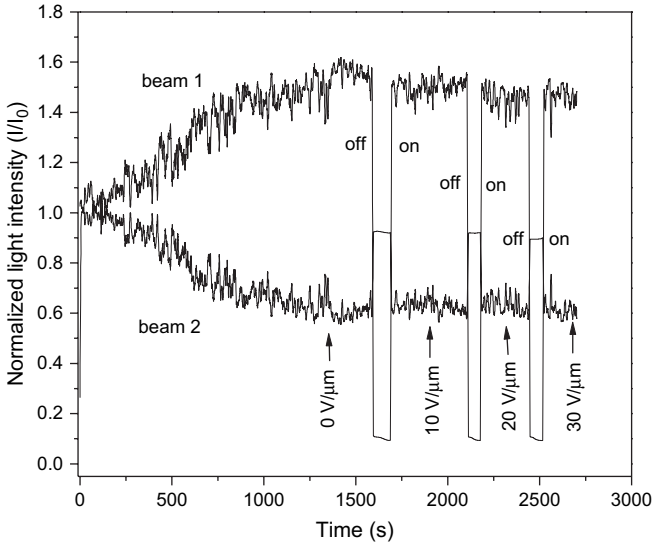

Fig. 5. Energy transfer in TBC experiment of **P5** doped with 10% ECZ at different electric fields. The voltage applied over the sample was increased from 0 to 30 V/μm by increments of 10 V/μm. Off and on refer to beam 1 turns off and on, respectively.

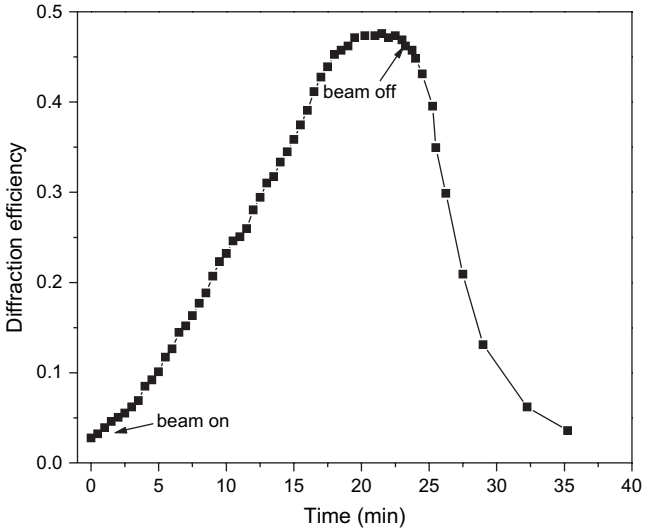

Fig. 6. Diffraction efficiency of the grating as a function of time for **P5** doped with 10% ECZ without external electric field. Beam on and off refer to beam 2 turns on and off, respectively.

response and an increase in photoconductivity. However, at temperature above T_g, while the PR dynamics can still improve, thermal disruption of the chromophore alignments and reduced trap densities lead to a deteriorated steady-state performance [1]. Therefore, it is reasonable to expect improved PR properties by tuning the T_g of materials close to experimental temperature (room temperature in our case).

As a common approach to tune the T_g, a polymer composite was prepared by doping polyphosphazene **P5** with a charge-transporting plasticizer, *N*-ethyl carbazole (ECZ). The T_g of a composite of **P5**/ECZ (90/10 wt%) was measured as 23 °C by DSC and no crystallization occurred during the heating and subsequent cooling processes. Fig. 5 displays the typical TBC behavior of the composite at zero electric field and different external fields. A large stable energy coupling between two writing beams was observed at zero electric field and a gain as high as 198 cm^{-1} was achieved. However, the writing time for the present grating was relatively slow, possibly due to reduced photogeneration efficiency or slow photogeneration resulting from the lack of an extra photo-sensitizer. Furthermore, the low photogeneration efficiency would likely give rise to an already saturated internal space-charge field at zero external field, which would give a possible explanation to the fact that the measured TBC gain derived from space-charge field did not vary significantly with increase of external fields as shown in Fig. 5. The FWM experiment was also performed without external electric field and the diffraction efficiency as function of time is shown in Fig. 6. It seems that both forming and erasing process of the grating need a longer time and the stable-state diffraction efficiency was measured to be 46%.

The steady-state PR performance of **P5** was enhanced significantly by adding the plasticizer ECZ to lower the T_g, which could be ascribed to improved orientational properties and therefore higher EO response. For the single-component sample **P7**, which has the lowest T_g, the longer inert alkylene chain between the side group and the phosphazene backbone act as an internal plasticizer in fact. While the internal inert plasticizer seems more efficient in lowering the T_g, problems are often encountered with general dilution of functional moieties and the interruption of charge transport. ECZ, as an excellent charge-transporting plasticizer, may fill the interspaces of macromolecules and come in being a network of charge transport to provide higher mobility, which would lead to an enhanced internal space-charge field and consequently the increase of the photorefractivity. Besides, ECZ has a good compatibility with the host polymer **P5** since it contains the same carbazole group of the host polymer, and the obtained low T_g composite sample do not show any phase separation and maintain the optical quality for at least one year.

4. Conclusion

A series of photorefractive polyphosphazenes containing carbazole-based multifunctional chromophores were prepared. Due to the highly flexible character of the phosphazene backbone and the flexible spacer group, the polymers show low glass transition temperature (20–65 °C) and have excellent solubility in common organic solvents, which can easily be fabricated into an optically transparent film with long-term stability. The effects were explored of variations in the length of the alkylene spacer between the side groups and the polymer backbone on the glass transition temperature, chromophore loading, as well as the optical gain. All of these single-component polymers exhibited PR performance at room temperature without external electric field or prepoling and gain coefficient of 91 cm^{-1} was observed in the polymer **P7** with the lowest glass transition temperature. When an external electric field was applied to these single-component

polymers, the optical gain reduced at the beginning, and then increased gradually with the external electric field. The steady-state PR performance of polymer **P5** was enhanced significantly by adding a photoconductive plasticizer ECZ to lower the T_g and a gain of 198 cm^{-1} and a diffraction efficiency of 46% were achieved at zero electric field. The fact that neither a prepoling process nor an external electric field is necessary for photorefractivity in the polymers would be of great advantage over conventional photorefractive polymers for practical applications.

Acknowledgments

We are grateful to the financial supports from the National Natural Science Foundation of China (project no. 20274042) and Henan Provincial Government of China (project 2005HANCET-11).

References

[1] Ostroverkhova O, Moerner WE. Chem Rev 2004;104:3267.
[2] Moerner WE, Jepsen AG, Thompson CL. Annu Rev Mater Sci 1997;27:586.
[3] Suh DJ, Park OO, Ahn T, Shim HK. Jpn J Appl Phys 2002;41:L428.
[4] Joo WJ, Kim NJ, Chun H, Moon IK, Kim N. Polymer 2001;42:9863.
[5] You W, Cao SK, Hou ZJ, Yu LP. Macromolecules 2003;36:7014.
[6] Wang Q, Wang LM, Yu LP. Macromol Rapid Commun 2000;21:723.
[7] Zhang YD, Wada T, Wang LM, Aoyama T, Sasabe H. Chem Commun 1996:2325.
[8] Ho MS, Barrett C, Paterson J, Esteghamation M, Natansohn A, Rochon P. Macromolecules 1996;29:4613.
[9] Barrett C, Choudhury B, Natansohn A, Rochon P. Macromolecules 1998;31:4845.
[10] Shi J, Huang MM, Chen ZJ, Gong QH, Cao SK. J Mater Sci 2004;39:3783.
[11] Shi J, Jiang ZW, Cao SK. React Funct Polym 2004;59:87.
[12] Shi J, Jiang ZW, Zhang L, Cao SK. Chin J Polym Sci 2004;22:551.
[13] Allcock HR, Mang MN, Dembek AA. Macromolecules 1989;22:4179.
[14] Allcock HR, Ravikiran R, Olshavsky MA. Macromolecules 1998;31:5206.
[15] Allcock HR, Dembek AA, Kim C, Devine RLS, Shi Y, Steier WH, et al. Macromolecules 1991;24:1000.
[16] Olshavsky MA, Allcock HR. Macromolecules 1995;25:6188.
[17] Li Z, Li J, Qin JG. React Funct Polym 2001;48:113.
[18] Zhang L, Huang MM, Jiang ZW, Yang Z, Chen ZJ, Gong QH, et al. React Funct Polym 2006;66:1404.
[19] De Jaeger R, Gleria M. Prog Polym Sci 1998;23:179.
[20] Zhang L, Yang Z, Jiang ZW, Shi J, Cao SK. J Funct Polym 2005;18:630 [in Chinese].
[21] Iftime G, Labarthet FL, Natansohn A, Rochon P, Murti K. Chem Mater 2002;14:168.
[22] Cheben P, Monte F, Worsfold DJ, Carlsson DJ, Grover CP, Mackenzie JD. Nature 2000;408:64.
[23] Hattemer E, Zentel R, Mecher E, Meerholz K. Macromolecules 2000;33:1972.
[24] Chen YW, He YK, Wang F, Chen HY, Gong QH. Polymer 2001;42:1101.
[25] Kim D, Tripathy S, Li L, Kumar J. Appl Phys Lett 1995;66:1166.
[26] Mun J, Lee JW, Park JK, Lee KS, Yoon CS. Opt Mater 2002;21:379.
[27] Chang CJ, Wang HC, Liao GY, Whang WT, Liu JM, Hsu KY. Polymer 1997;38:5063.
[28] Lee JW, Mun J, Yoon CS, Lee KS, Park JK. Adv Mater 2002;14:144.
[29] Sekkat Z, Dumont M. Appl Phys B 1992;54:486.
[30] Sekkat Z, Wood J, Aust EF, Knoll W, Volksen W, Miller RD. J Opt Soc Am B 1996;13:1713.
[31] Enomoto T, Hagiwara H, Tryk DA, Liu ZF, Hashimoto K, Fujishirma A. J Phys Chem B 1997;101:7422.
[32] Simoni F, Cipparrone G, Mazzulla A, Pagliusi P. Chem Phys 1999;245:429.
[33] Cipparrone G, Mazzulla A, Pagliusi P. Opt Commun 2000;185:171.
[34] Huang MM, Chen ZJ, Gong QH, Shi J, Cao SK. Chin Phys Lett 2006;23:2468.